ELSEVIER

Biophysical Chemistry 93 (2001) 181–196

Biophysical Chemistry

www.elsevier.com/locate/bpc

Crystallohydrodynamics for solving the hydration problem for multi-domain proteins: open physiological conformations for human IgG

Beatriz Carrasco[a], Jose Garcia de la Torre[a], Kenneth G. Davis[b,c], Susan Jones[d], Diljeet Athwal[e], Chris Walters[c], Dennis R. Burton[b,f,g], Stephen E. Harding[c,*]

[a] *Departamento de Quimica Fisica, Facultad de Quimica, Universidad de Murcia, 30071 Murcia, Spain*
[b] *Krebs Institute, Department of Molecular Biology and Biotechnology, The University, Sheffield S10 2TN, UK*
[c] *National Centre for Molecular Hydrodynamics, University of Nottingham, School of Biosciences, Sutton Bonington LE12 5RD, UK*
[d] *Biomolecular Structure and Modelling Unit, Department of Biochemistry and Molecular Biology, University of London, Gower Street, London WC1 6BT, UK*
[e] *Celltech Therapeutics, Bath Road, Slough, Berkshire SL1 4EN, UK*
[f] *Department of Immunology, The Scripps Research Institute, North Torrey Pines Road, La Jolla, CA, USA*
[g] *Department of Molecular Biology, The Scripps Research Institute, North Torrey Pines Road, La Jolla, CA, USA*

Received 15 May 2001; received in revised form 1 July 2001; accepted 20 July 2001

Abstract

Hydrodynamic methods provide a route for studying the low-resolution conformation — in terms of time-averaged spatial orientation of the Fab′ and Fc domains relative to each other — of the human IgG subclasses, IgG1, IgG2, IgG3 and IgG4 in the environment in which many exist naturally — a solution. Representative modelling strategies are now available using 'shell-bead' or 'shell' modelling of the surface of the molecules with the size-independent programme SOLPRO [J. Garcia de la Torre, S.E. Harding, B. Carrasco, Eur. Biophys. J. 28 (1999) 119–132]. The shell model fits to the equivalent inertial surface ellipsoids of the published crystal structures for the Fab′ and Fc domains of IgG are made and an apparent hydration δ_{app} of 0.51g/g for Fab′ and 0.70 g/g for the glycoprotein Fc are obtained, which yield an average value of (0.59 ± 0.07) g/g for the intact antibody (2 Fab′ + 1 Fc). The relative orientations of these domains for each of the IgG subclasses is then found (using where appropriate a cylindrical hinge) from SOLPRO by modelling the Perrin function, P (i.e. 'frictional ratio due to shape') using this δ_{app} and experimentally measured sedimentation coefficients. All the IgG subclasses appear as open, rather than compact

* Corresponding author. Tel.: +44-115-951-6148; fax: +44-115-951-6142.
E-mail address: steve.harding@nottingham.ac.uk (S.E. Harding).

PII: S0301-4622(01)00220-4

structures with the degree of openness IgG3 > IgG1 > (IgG2, IgG4), with IgG3 and IgG1 non-coplanar. The hingeless mutant IgGMcg, with $s^{\circ}_{20,w} \sim 6.8$ S yields a coplanar structure rather similar to IgG2 and IgG4 and consistent with its crystallographic structure. The extension of this procedure for representing solution conformations of other antibody classes and other multi-domain proteins is indicated.

Keywords: Human IgG; Crystallohydrodynamics; Proteins; Hydration

1. Introduction

The representation by molecular hydrodynamic techniques of the low-resolution conformation of IgG and other classes of antibody in an environment in which many exist naturally — a dilute solution — has in the past proved difficult. Ellipsoid shapes per se — whose hydrodynamic properties can be described without error [1–3] — are applicable only for representing the individual domains (Fab, Fab′ or Fc), and not the complete structure. The representation of solution structures as a multiple array of spheres — known as bead modelling ([4] and references therein), and, in particular, the *surface* of the solution structure as an array of tiny beads — known as bead-shell or just 'shell' modelling [5] — offers a realistic alternative. Simple bead models were the first to indicate that IgE has a bent or cusp-shape conformation in solution [6].

Although the hydrodynamic parameters for a multi-body array of spherical beads can be calculated only approximately, recent advances in both theory and computational procedures mean that for *most parameters* (with the possible exception of the viscosity increment) they can generally be calculated to an accuracy better than that of the experimental error so long as so-called 'filling models' are avoided [5]. Carrasco and Garcia de la Torre [5] have recently performed an exhaustive comparison of such procedures. Those involving the bead-shell approach appear particularly attractive, and such an approach has recently been successfully applied to representing an ellipsoidal surface based on published crystallographic structure(s) for the IgG Fab′ domain [7]. Combining the experimentally measured translational frictional ratio f/f_0 (the ratio of the frictional ratio of the macromolecule to that of a sphere of the same mass and anhydrous volume) — a ratio that can be obtained from the sedimentation coefficient, molecular weight and partial specific volume — with the Perrin function P (or 'translational frictional ratio due to shape') calculated from the bead shell model to the crystallographic ellipsoidal surface, provides an estimate of $\sim 0.51 \pm 0.07$ g/g for the apparent hydration, δ_{app}, of the Fab′ model. (By 'apparent hydration', we mean, following Gregory et al. [10] its value may be affected by inexactness of the bead model fit to the true structure.) The Perrin function (see e.g. Squire and Himmel [8]) is a universal shape parameter totally independent of size and is represented by the symbol P in recognition of F. Perrin who provided a complete formulation of this for general ellipsoids in 1936 [9]. The translational frictional ratio f/f_0 thus has two molecular contributions — one from shape (represented by the parameter P) — and one from volume (which includes hydration).

After performing a similar representation (to that described previously for Fab′ [7]) for the ellipsoid Fc domain, the bead shell approach allows us the possibility of assembling the domains together (with the addition, where appropriate, of a cylindrical hinge region represented as a surface of beads), to assess the time-averaged angles between the domains in solution that are consistent with the observed hydrodynamic properties. Such a description is shown schematically in Fig. 1.

Using values for the apparent hydration found previously for Fab′ [7] and in the current study also Fc, together with bead-shell model fits to the ellipsoidal domain surfaces we will attempt piecing together the intact human IgG molecule in such a way as to reproduce the observed sedimen-

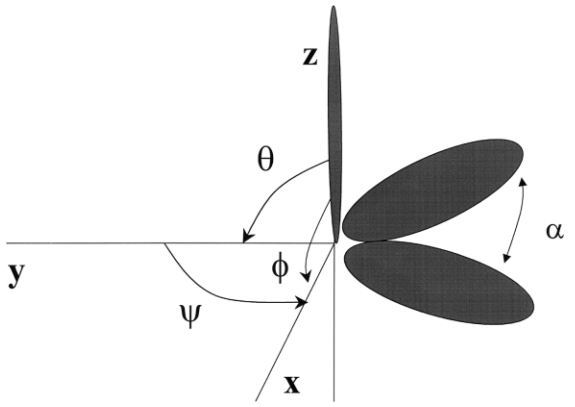

Fig. 1. Orientation angles between Fab′ and Fc domains relative to an *xyz* Cartesian frame. α, angle between Fab domains; θ, non-coplanarity angle of the Fc domain to the Fab′s; θ = 90° corresponds to a planar structure; ϕ, twist angle (swivel of the Fc face); ψ, bend angle (bending up of Fc towards one of the Fab arms).

tation properties for its subclasses IgG1, IgG2, IgG3, IgG4 and the hingeless, immunologically inactive mutants IgGDob and IgGMcg.

1.1. Earlier bead models of IgGs

Gregory et al. [10] used conventional bead modelling to represent the solution conformation of the IgG subclasses based on the following strategy: (1) Use the published crystallographic structure of the hingeless mutant IgG known as IgGDob [11,12]. (2) Use a simple arrangement of six beads (two each for Fc and the two Fab′s) to represent the IgGDob structure. (3) Calculate the 'translational frictional ratio due to shape' using the programme GENDIA [13]. (4) Compare with the experimentally measured sedimentation coefficient $s^{\circ}_{20,w}$ of 6.3 S to evaluate an apparent hydration δ_{app} of 0.95g/g. (5) For experimental values of 6.6 S of IgG1, 6.95 S for IgG2, 5.9 S for IgG3 and 6.4 S for IgG4, explore what combination of α (angle between the Fab arms), 'non-coplanarity angle(s)' — see Fig. 1, and, in the case of IgG1 and IgG3, hinge length *h*, would reproduce the same apparent hydration δ_{app} of 0.95 g/g as IgGDob, as manifested in a comparison of the theoretical with experimental sedimentation coefficients. Essentially this strategy of Gregory et al. [10] indicated that the observed sedimentation coefficients were consistent with:

1. IgG1: a hinge length of 0–15 Å and non-coplanar arms;
2. IgG2: effectively hingeless with folded back Fab arms;
3. IgG3: has an extended hinge of ~ 100 Å and is non-coplanar; and
4. IgG4: is effectively hingeless, and, like IgGDob, T-shaped.

Attempts were also made for IgG1 and IgG3 to support these observations with small-angle X-ray scattering determinations of the root mean square radius of gyration, R_g. This yielded values for R_g lower than earlier evaluations of R_g [14,15], differences ascribed to possible aggregation problems: the considerably higher concentrations required (up to 10 mg/ml) compared with sedimentation analysis in the ultracentrifuge, together with beam damage and the propensity for these proteins to aggregate were proposed as causes for the disagreement. The differential sedimentation properties between the IgG subclasses and IgGDob remained the main experimental cornerstone for the models.

1.2. Problems with IgGDob

The models of Gregory et al. [10] are totally dependent on the experimental sedimentation coefficient $s^{\circ}_{20,w} = 6.3$ S for IgGDob. A subsequent source of doubt was the rather low value of this in relation to other published data for other IgG antibodies (IgG2, IgG4) of similar molecular weight and without a significant hinge region. A further doubt was the rather high value for the apparent hydration δ_{app} for IgGDob (0.95 g/g) which is considerably in excess of the estimated range [8] of 0.2–0.7 g/g for proteins (and glycopolymers of modest degree of glycosylation).

1.3. A refined strategy

We can now take advantage of recent advances in hydrodynamic modelling to give a more refined

description of the solution conformation of these substances, particularly with regard to bead-shell modelling and the employment of universal shape of parameters. Universal shape parameters [1,3,24] are shape parameters independent of molecular size. So the Perrin 'frictional ratio due to shape' function P is a universal parameter since a given shape has a single value of P, whereas the sedimentation coefficient is not, since the value of the latter is affected by the molecular weight and volume (including hydration contributions) of the macromolecule.

The 'crystallohydrodyamic' strategy to evaluate the low-resolution structure of an antibody molecule in terms of the time-averaged spatial orientation of its Fab and Fc domains relative to each other is essentially as follows. Crystal structure of domains + Hydrodynamic measurements of domains + Hydrodynamic measurements of intact antibody → Low resolution structure (relative domain orientation) of intact antibody

Essentially the combination of the crystal structural with the hydrodynamic information for the domains provides an estimate for the (time averaged) hydration of the domains. Since the domain composition of antibodies are known (generally 2 Fabs′ + 1 Fc), the average hydration of the intact antibody can then be specified: this combined with hydrodynamic measurements on the intact molecule then leads to the conformation of the latter.

The details of the procedure for the present application to IgG subclass structure determination are as follows.

1. Represent the surface of the Fc domains by an inertial ellipsoid fit using a version of the ELLIPSE algorithm [16] implemented by Hubbard [17], and a second algorithm SURFNET [18] and use the results of a recently published fit for IgG Fab′ [7] using the same procedure. This specifies values for the two axial ratios (a/b, b/c) describing the shape of the surface (Fig. 2).
2. Evaluate the value of the shape function P exactly by entering the values for (a/b, b/c) into the routine ELLIPS2 [3] which employs the exact hydrodynamic relations for general ellipsoids.
3. Represent the surface of each domain with a bead-shell model (rather than the two to three large spheres used by Gregory et al. [10]).
4. Evaluate the experimental translational frictional ratio (f/f_0) for Fc following the same procedure used previously for Fab′ [7] by measuring the sedimentation coefficient, molecular weight and partial specific volume and using the relation

$$(f/f_0) = M(1-\bar{v}\rho_0)/\left[N_A 6\pi\eta_0 s^{\circ}_{20,w} \times\{(3\bar{v}M)/(4\pi N_A)\}^{1/3}\right] \quad (1)$$

where M is the molecular weight (g/mol), $\bar{v}$

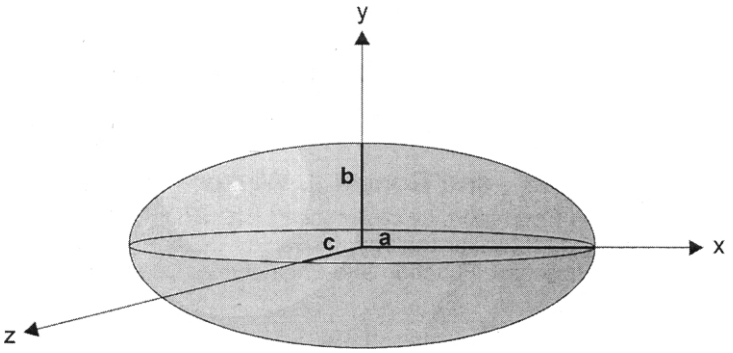

Fig. 2. General triaxial ellipsoid. Semi-axes $a \geq b \geq c$, axial ratios (a/b, b/c). The hydrodynamic properties for this can be specified exactly.

the partial specific volume (ml/g), N_A is Avogadro's number (6.02×10^{23} mol^{-1}), $s^{\circ}_{20,w}$ the sedimentation coefficient (s) corrected to the standard conditions of density (ρ_o, g/ml) and viscosity (η_o, Poise) of water at 20.0°C, and extrapolated to infinite dilution [19].

5. Evaluate the apparent hydration δ_{app} for Fc following the same procedure used for Fab′ [7], i.e. combining P evaluated in '2' above, with the experimentally measured translational frictional ratio using the relation [8,7]

$$\delta_{app} = \left\{[(f/f_0)/P]^3 - 1\right\}\bar{v}\rho \quad (2)$$

.

6. Estimate δ_{app} for the intact antibodies based on the values for Fc and Fab′ and the domain composition (2 Fab′ + 1 Fc).
7. For each antibody subclass evaluate the experimental translational frictional ratio (f/f_0) from Eq. (2).
8. For each IgG subclass evaluate the experimental 'translational frictional ratio due to shape', or Perrin function P, from a rearranged form of Eq. (2):

$$P = (f/f_0)\left\{1 + \left(\delta_{app}/\bar{v}\rho_0\right)\right\}^{-1/3} \quad (3)$$

9. For each IgG subclass find the appropriate combination(s) of orientations (Fig. 2) between the Fab′ and Fc domains that give a theoretical P value from SOLPRO that best reproduces the experimental P value.

2. Triaxial bead shapes for Fab′, Fab and Fc

The triaxial shape, in terms of a general ellipsoid (Fig. 2) of semi-axes ($a \geq b \geq c$) and axial ratios (a/b, b/c), for a range of IgG Fab′ and Fab domains has recently been described by Carrasco et al. [7]. The procedure followed was that of Taylor et al. [16] which is insensitive to small deviations from ideal ellipsoid form, and is based on the inertial, momental or 'Cauchy' ellipsoid [20,21] dilated so that it forms a close approximation to the protein surface. The original procedure, recently implemented by Hubbard [17] in a FORTRAN program, is used to calculate the ratios of the principal axes of the equi-momental ellipsoid for the three-dimensional co-ordinates of the protein. These ratios can be used in conjunction with a second algorithm SURFNET [18] to generate a three-dimensional surface representation of the ellipsoid. Carrasco et al. [7] obtained a value for the axial ratios (a/b, b/c) of (1.60, 1.42) based on the crystallographic structure of a chimeric IgG Fab′ [22] (Fig. 3a) and found little variation between this and a chimeric Fab lacking the hinge (a/b, b/c) = (1.65, 1.40), and also human Fab (1.59, 1.36) and murine Fab (1.68, 1.39).

We can now attempt the same for human Fc, based on the published crystal co-ordinates of an Fc fragment [23]. Fig. 3b shows a fit to the crystal structure and values for (a/b, b/c) of (1.10, 1.85) are obtained: the Fc domain is clearly more discoid (oblate) compared with the Fab′/Fab domains. The corresponding semi-axial dimensions for the Fab′ and Fc are given in Table 1.

2.1. Construction of corresponding bead models

We follow the procedure of Carrasco et al. [7] for Fab′ and now apply this to Fc. To facilitate the construction of the shell model, the equivalent ellipsoid of revolution is first defined (by setting $b = c$ or $a = b$). In the case of Fab′ this gave a revised (a/b, b/c) of (1.83, 1.00) — i.e. a prolate ellipsoid: this approximation is justified since it led to error of only ~1% in the frictional based P function. For Fc this will be an oblate ellipsoid of (a/b, b/c) = (1.00, 1.95). In this case the P function of 1.039 evaluated for a triaxial ellipsoid (a/b, b/c) = (1.10, 1.85) is identical to that for an oblate ellipsoid of a/b, b/c) = (1.00, 1.95). Fig. 4a shows the bead shell approximation to the surface of the ellipsoid for Fab′ [7] and Fig. 4b the corresponding representation for Fc.

The procedure for arranging the beads is as follows: a number of small beads of radius σ are placed in such a way that their centres lie on the surface of the ellipsoid. Each bead is touching its closest neighbours, or closely tangent with them, with small gaps. The number of beads, N, is large and increases with decreasing σ; for instance, for

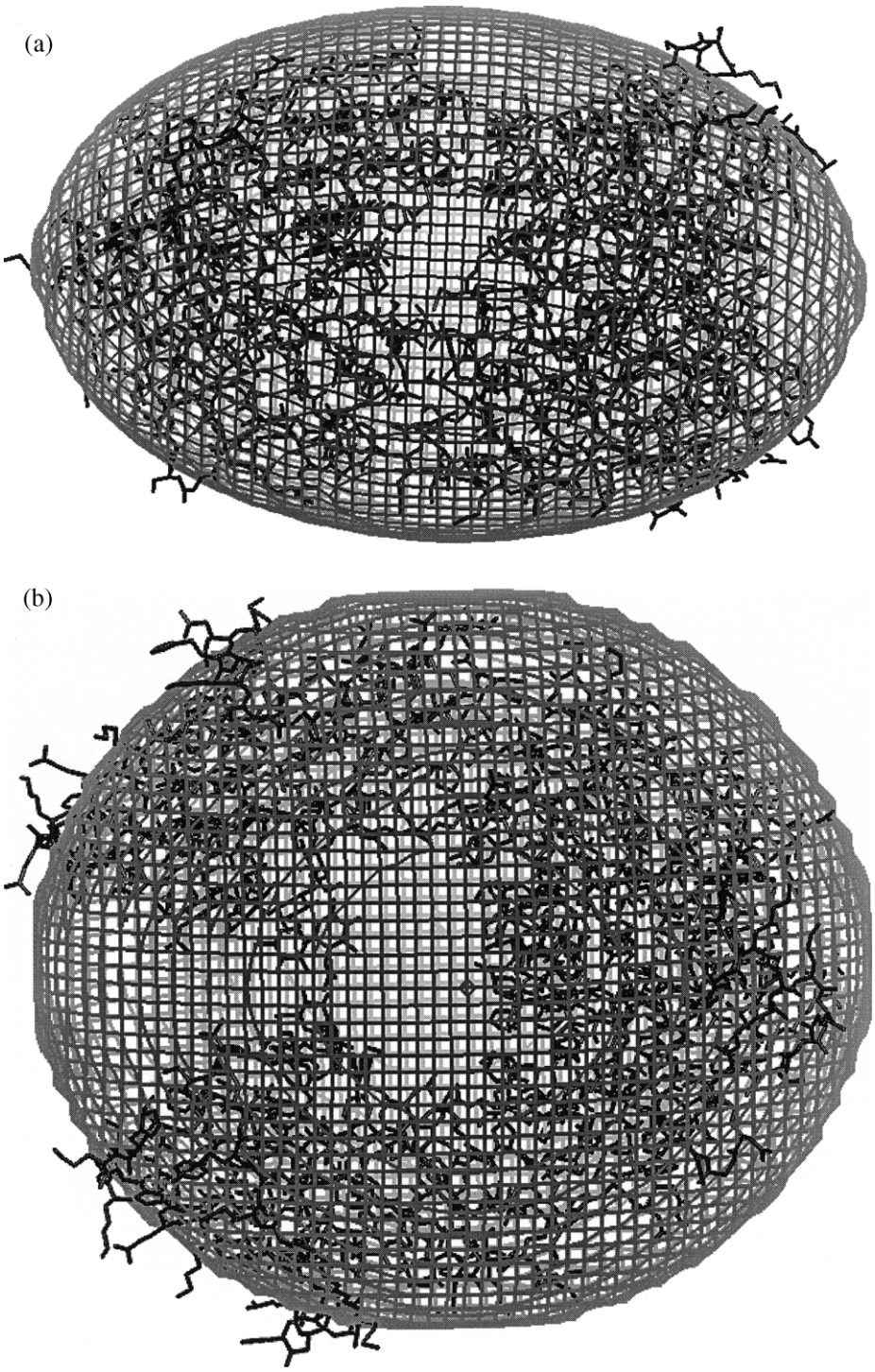

Fig. 3. General triaxial shape fits to the surface of the crystal structures of (a) IgGFab′ and (b) IgGFc using PROTRUDER and SURFNET. The hydrodynamic properties of the fitted triaxial ellipsoids can be exactly described by the ELLIPS2 programme.

Table 1
Triaxial shape and semi-axial dimensions ($a \geq b \geq c$) for human IgG Fab′ and Fc from crystal structures

	(a/b, b/c)	(a, b, c) Å	PDB file	Reference
Fab′ (B72.3c)	1.60, 1.42	56.7, 35.6, 23.1	1bbj 3.1 Å	Brady et al. [22]
Fc	1.10, 1.85	51.5, 46.7, 25.2	1fc1 2.9 Å	Deisenhoffer [23]

the smallest radius considered in our calculations, $\sigma = 1.64a$ (which is a fraction $0.033a$ of the longest semi-axis, $a = 49.1$ Å of the ellipsoid), we have $N = 1910$. The computing time for the HYDRO calculation of the shell model grows as N^3. Actually, we have made the calculations for various bead sizes, ranging from $0.086a$ to $0.033a$. The resulting properties show a slight dependence on σ; the final results are obtained by extrapolating to the shell model limit of $\sigma = 0$. This is done by fitting the data to a polynomial of degree 1 or 2, depending on the cases involved. The hydrodynamic parameters such as P can then be evaluated using HYDRO/SOLPRO according to the procedures described in Garcia de la Torre et al. [24,25], and hence δ_{app} can be specified from Eq. (3) once the experimental (f/f_0) is known for Fc, exactly as was done previously for Fab′ [7].

3. Experimental methods

3.1. Fc

The Fc fragment used in the present study was prepared by digestion of a human IgG1 antibody using immobilised papain, [26] to release the Fc portion of the antibody. The Fc fragment was purified by first loading the digest, following removal of the papain, over a protein A column. Fc protein was eluted from the column with citric acid pH 3.0. The eluate was further passed over a protein L column to remove antibody contaminants and any undigested antibody. The Fc sample was neutralised with Tris pH 6.

3.2. IgG subclasses

Human myeloma proteins of the IgG2 and IgG4 subclasses were prepared from serum by standard procedures as described by Burton et al. [27]. The hinge deleted IgGDob was a kind gift from Drs S.K. Dower and D.M. Segal and the hinge deleted IgGMcg was a kind gift from Dr Alan Edmundson.

3.3. Solutions for ultracentrifuge experiments

All experiments were carried out on proteins in 0.15 M KCl/0.02 M potassium phosphate buffer

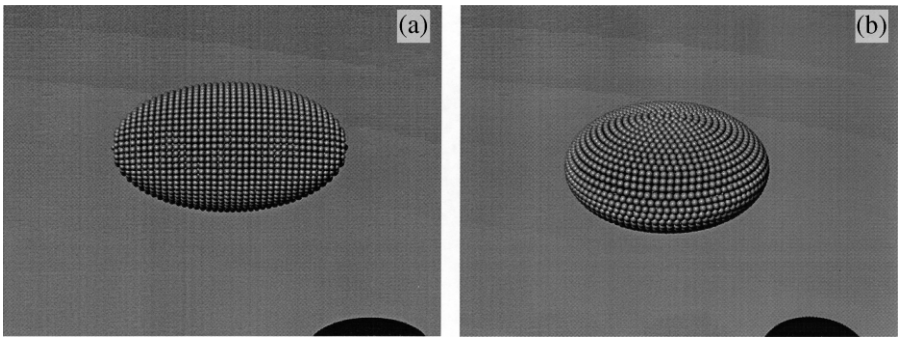

Fig. 4. Bead shell models for (a) the equivalent prolate ellipsoid fit to Fig. 3a for IgGFab′ and (b) the equivalent oblate ellipsoid fit to Fig. 3b for IgGFc.

(pH 7.0), as previously used by Gregory et al. [10]. Concentrations were determined by absorbance measurement using an extinction coefficient at 280 nm for a 1 mg/ml solution of 1.5 [10]. Protein purity was assessed by SDS-PAGE and protein concentrations (needed only for extrapolation of the sedimentation coefficient to infinite dilution) were determined by absorbance measurements using an extinction coefficient of 1500 ml g^{-1} cm^{-1} [10]. Protein purity was confirmed by SDS-PAGE.

3.4. Sedimentation velocity analysis in the analytical ultracentrifuge

Beckman Optima XL-A [28] and MSE Centriscan ultracentrifuges were used, both equipped with scanning ultraviolet absorption optics, with the monochromator set at a wavelength of 280 nm. All experiments were performed at a temperature of 20.0°C.

Sedimentation coefficients in the buffer at 20.0°C, $s_{T,b}$ were evaluated using SVEDBERG [29], LAMM [30] and DCDT [29,31], or simple boundary analysis (SEDVEL). The first three routines also yield estimates for the translational diffusion coefficient $D_{T,b}$. $s_{T,b}$ values were corrected to standard solvent conditions (density, ρ_o and viscosity η_o of water at 20.0°C, using the formula [19]

$$s_{20,w} = \{(1-\bar{v}\rho_0)_{20,w}/(1-\bar{v}\rho_0)_{T,b}\} \times \{\eta_{T,b}/\eta_{20,w}\}s_{T,b} \quad (4a)$$

The partial specific volume $\bar{v}$ for Fc and the IgG subclasses was calculated from the amino acid sequence and carbohydrate composition using the consensus formula of Perkins [32]. A similar correction was employed for the translational diffusion coefficient:

$$D_{20,w} = (293.15/T)\{\eta_{T,b}/\eta_{20,w}\}D_{T,b} \quad (4b)$$

$s_{20,w}$ values were plotted against sedimenting concentration (corrected for radial dilution) and extrapolated to infinite dilution according to the method of Gralén [33]

$$s_{20,w} = s^\circ_{20,w}(1-k_s c) \quad (5a)$$

where k_s is the Gralén [33] parameter. A similar extrapolation was performed to obtain the translational diffusion coefficient at infinite dilution, $D^\circ_{20,w}$

$$D_{20,w} = D^\circ_{20,w}(1-k_D c) \quad (5b)$$

4. Experimental results

Analytical ultracentrifuge experiments confirmed the purity of the 5 proteins studied (Fc, IgG2, IgG4, IgGDob, IgGMcg) from the shape and symmetry of the sedimenting boundaries. Fig. 5a shows the apparent distribution $g^*(s)$ vs. $s_{T,b}$ plot for human Fc from the program DCDT+ [29] and Fig. 5b the corresponding plot of $s_{20,w}$ vs. c yielding an $s^\circ_{20,w}$ of 3.85 ± 0.05 S.

Sedimentation equilibrium analysis using 'MSTARA' [34] yielded a weight average molecular weight, M_w of 52000 ± 1500 g/mol for the molecular weight of IgG1 Fc, in exact agreement with the sedimentation diffusion result: combining the $s^\circ_{20,w}$ of 3.84 ± 0.07 S and $D^\circ_{20,w}$ of $6.6 \pm 0.3 \times 10^{-7}$ cm^2 s^{-1} via the Svedberg equation:

$$M_w = \{s^\circ_{20,w}/D_{20,w}\}\{RT/(1-\bar{v}\rho)\} \quad (6)$$

where R is the gas constant, yielded a value for M_w of 52000 ± 2500 g/mol.

Table 2 gives the evaluated $s^\circ_{20,w}$ for Fc together with IgG1–IgG4 and the mutants IgGDob and IgGMcg. For the IgG subclasses, the criterion for making fresh measurements in this study was if there was less than one previous study supporting a particular measurement. In the case of IgG1 and IgG3 more than one study was available supporting a particular value: this was not the case for IgG2 and IgG4. The result in the present study of $s^\circ_{20,w} = 6.76 \pm 0.04$ S for IgG2 appears to confirm the value of 6.8 S of Kilar et al. [15] but is somewhat lower than that of 6.95 ± 0.10 S of Gregory et al. [10]. The result in the present study of $s^\circ_{20,w} = 6.73 \pm 0.06$ S for IgG4 — very similar to that for IgG2, but somewhat higher

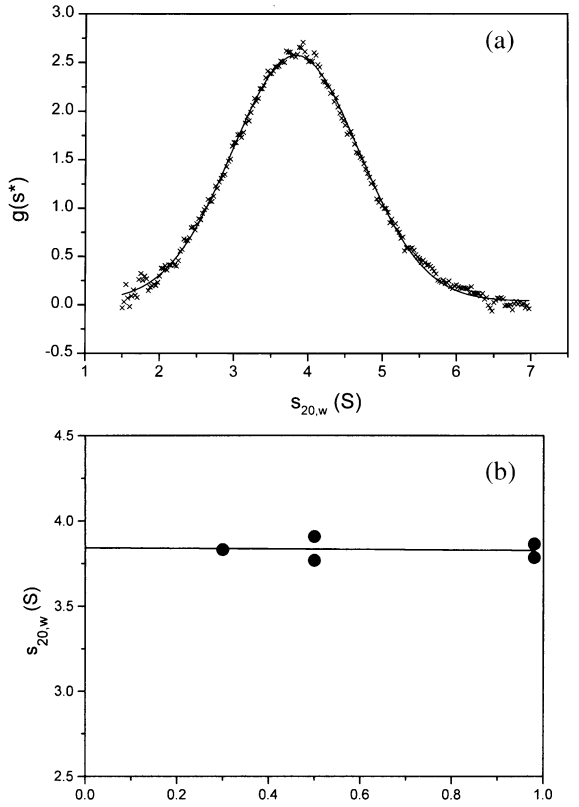

Fig. 5. (a) $g(s^*)$ vs. $s_{20,w}$ plot from the programme DCDT+ [29] for IgGFc. Loading concentration 0.5 mg/ml. Rotor speed = 50000 rev./min, temperature = 20.0°C. $g(s^*)$ is the apparent (i.e. not corrected for diffusion) distribution of sedimentation coefficients. (b) Gralén plot of $s_{20,w}$ vs. sedimenting concentration, c.

than the previous value of 6.40 ± 0.05 S of Gregory et al. [10]. The latter value may have been due to some chain dissociation. The value for IgGMcg of 6.79 ± 0.10 S is similar to that of IgG2 and IgG4 but in disagreement with another hingeless mutant, IgGDob. Surprisingly the 'low' value obtained previously of 6.30 ± 0.05 S by Gregory et al. [10] was confirmed. This particular finding for IgGDob is further discussed below.

4.1. Experimental translational frictional ratios

In Table 3 we have calculated the experimental translational frictional ratios from Eq. (1) and using consensus values for the sedimentation coefficient, together with values for $\bar{v}$ evaluated from the amino acid and carbohydrate composition data.

4.2. Apparent hydration of human IgG Fc and comparison with Fab'

For IgG Fc, taking $\bar{v} = 0.730$ ml/g (from the amino acid sequence), $M = 51\,019$ g/mol, and $s^{o}_{20,w} = 3.85 \pm 0.05$ S (η and ρ are the viscosity and density of water at 20°C and N_A is Avogadro's number), we calculate $f/f_0 = 1.29 \pm 0.02$ from Eq. (1). Taking the value of $P = 1.039$ from the bead model fit to the crystallographic/ellipsoid shape we then obtain from Eq. (2) a value for the hydration $\delta_{app} = 0.70$ for Fc, where the 'apparent' refers to the fact we have used the P value for the bead model which may be somewhat different for the actual protein [7].

For the appropriate δ_{app} of an intact IgG antibody we take the weighted average based on 2 Fabs and 1 Fab in an intact molecule, and obtain $\delta = 0.59$ for the 'consensus' value for intact IgG.

4.3. Experimental Perrin functions for the IgG subclasses

Using the consensus value of 0.59 g/g for δ_{app} calculated from a weighted average of the individual values for Fc and Fab', and assuming it is the

Table 2
Sedimentation coefficients for the major human IgG subclasses and fragments

Protein	$s^{\circ}_{20,w}$ (S)
IgGFab'	3.92 ± 0.01[e]
IgGFc	3.85 ± 0.07[a]
IgG1	6.60 ± 0.10[b,c]; 6.8[d]
IgG2	6.76 ± 0.04[a]; 6.95 ± 0.10[b]; 6.8[d]
IgG3	5.90 ± 0.10[b,c]; 6.3[d]
IgG4	6.73 ± 0.06[a]; 6.40 ± 0.05[b]
IgGDob	6.30 ± 0.05[a]; 6.30 ± 0.05[b]
IgGMcg	6.79 ± 0.10[a]

[a] This study.
[b] Gregory et al. [10].
[c] Schmidt-Kessen and Lustig [41].
[d] Kilar et al. [15].
[e] Carrasco et al. [7].

Table 3
Experimental translational frictional ratios and Perrin functions for the major human IgG subclasses and fragments

Protein	Consensus $s^{\circ}_{20,w}$ (S)	$\bar{v}$ (ml/g)	M (Da)	f/f_0	P (for $\delta_{app} = 0.59$)
IgGFab′	3.92 ± 0.01	0.727	47 499	1.22 ± 0.01	1.02 ± 0.01[a]
IgGFc	3.85 ± 0.05	0.730	51 019	1.29 ± 0.02	1.03 ± 0.02[b]
$(Fab')_2$	5.19 ± 0.03	0.727	94 996	1.46 ± 0.02	1.23 ± 0.02[a]
IgG1	6.60 ± 0.10	0.728	148 000	1.54 ± 0.03	1.26 ± 0.03
IgG2	6.76 ± 0.04	0.730	148 000	1.49 ± 0.03	1.22 ± 0.03
IgG3	5.90 ± 0.10	0.730	158 000	1.78 ± 0.04	1.46 ± 0.04
IgG4	6.73 ± 0.06	0.730	148 000	1.50 ± 0.02	1.23 ± 0.02
IgGDob	6.30 ± 0.05	0.730	145 000	1.58 ± 0.02	1.30 ± 0.02
IgGMcg	6.79 ± 0.10	0.730	145 000	1.46 ± 0.03	1.23 ± 0.03

[a] $\delta_{app} = 0.51$.
[b] $\delta_{app} = 0.70$.

same for the intact IgG subclasses we can convert the experimental translational frictional ratios into the Perrin functions P using Eq. (2), and this we have done in Table 3. It is interesting to note that, within experimental error the P values for the various IgG subclasses compare in the following way with each other: IgG3 > IgG1 > IgG4 > IgG2. The P value — which, unlike the sedimentation coefficient from which it is derived is independent of size and purely a measure of shape — is essentially a measure of openness of a structure, with lower limit of 1.0 for a sphere (hydrated or anhydrous). We will now attempt to be more specific in terms of the average orientation of the domains (Fig. 1).

5. Construction of bead shell models for $(Fab')_2$ and the intact IgG subclasses

5.1. $(Fab')_2$

This is the simplest case with only one angle (α) describing the orientation between the 2 Fab′ domains. Table 4 gives the various theoretical values from SOLPRO for various orientations of the domains (i.e. angles α). The maximum stretch angle ($\alpha = 180°$) gives a P value from SOLPRO ($P = 1.21$) closest to the experimental value ($P_{exp} = 1.23 \pm 0.03$). The corresponding shell model is given in Fig. 6.

Table 4
Simulated values for the Perrin function P for $(Fab')_2$, for various orientations α

α (°)	60	90	120	150	180
P	1.068	1.136	1.178	1.201	1.208

5.2. IgG1, IgG2, IgG4

Representations of the possible domain orientations of these antibodies with only a small (IgG1)

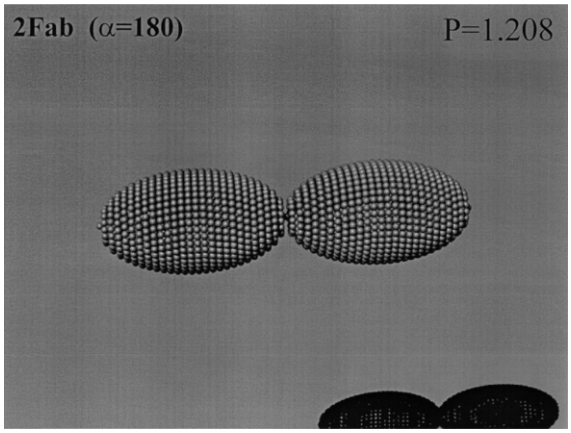

Fig. 6. Bead shell model for human $(Fab')_2$. Experimental Perrin function $P = (1.23 \pm 0.02)$. Modelled $P = 1.21$ (linear arrangement of domains: other arrangements give lower values).

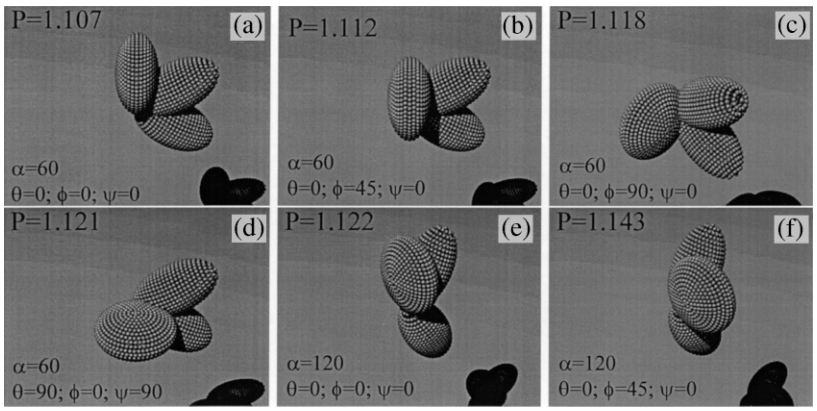

Fig. 7. These compact models for the intact human IgG1, IgG2 and IgG4 antibodies give model P values too small compared with the measured experimental value of (1.26 ± 0.03), (1.22 ± 0.03) and (1.23 ± 0.02) respectively, and are ruled out.

or very small (IgG2, IgG4) hinge regions are shown for a series of compact models (with domains folded inwards on each other) in Fig. 7. All of the compact models of Fig. 7 yield theoretical P values from SOLPRO that are too small, even allowing for experimental error. A satisfactory representation is achieved for more open models and a planar Y-model (with $\phi = 0°$, and an angle, $\alpha = 120°$ between the Fab arms) — giving $P = 1.23$ from SOLPRO for IgG4 (Fig. 8a), and the same Fab angle but a more distorted Y-shape ($\phi = 45°$) for IgG2 ($P = 1.22$, Fig. 8b) agreeing with the experimental (P_{exp}) values of 1.22 and 1.23. Within experimental error both of the models of Fig. 8 would be appropriate for IgG2 and IgG4, which are experimentally indistinguishable on the basis of the sedimentation (translational frictional) properties.

5.3. IgG1

For IgG1 we have allowed a small cylindrical hinge (length 15 Å and diameter 15 Å) and another open model with the same Fab angle gives a satisfactory fit (SOLPRO $P = 1.26$; $P_{exp} = 1.26$, Fig. 9a). Increasing the hinge length to 30 Å (Fig. 9b)we can still get the same agreement (SOLPRO $P = 1.26$) except that the Fc domain is moved through an angle of 45° towards either of the Fab arms. Although it could be argued that there

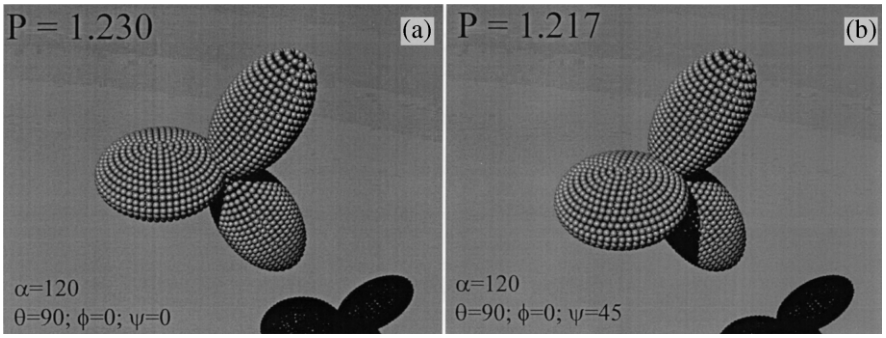

Fig. 8. Open Y-models for human IgG2 and IgG4. Experimental $P = 1.22 \pm 0.03$ for IgG2 and 1.23 ± 0.02 for IgG4. Experimentally it is impossible to distinguish these two subclasses on the basis of sedimentation properties alone. Model (a) ($P = 1.23$): coplanar Y shape; Model (b) ($P = 1.22$) distorted (non-coplanar) Y.

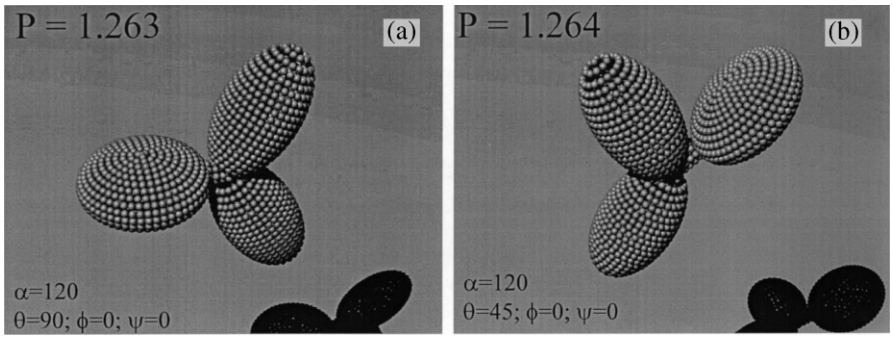

Fig. 9. Open Y-models for human IgG1. Small cylindrical hinge is necessary to model the experimental value of $P = 1.26 \pm 0.03$. Model (a). Coplanar hinged Y ($P = 1.263$); Model (b). Non-coplanar hinged Y ($P = 1.264$).

could be range of possible (α,θ,ϕ) angles, nonetheless only open structures give SOLPRO P values that are high enough.

5.4. IgG3

IgG3 has a hinge of some 70 residues with 11 interchain disulfide bridges. A variety of hinge lengths have been suggested, with the only direct visualisation estimate being that of Pumphrey et al. [35], who on the basis of electron microscopy, indicated the main body of the hinge to be approximately 90 Å long with a double helical arrangement of the two chains: various orientations of the domains with a cylindrical hinge of length/diameter ratio 6 (length = 90 Å, diameter = 15 Å) all give SOLPRO P which are somewhat smaller than the experimental $P_{exp} = 1.46 \pm 0.04$. To achieve agreement it is necessary to make the model even more open by increasing the length of the hinge region. An increase of $\sim 30\%$ to 120 Å yields the desired result (Fig. 10). In all cases the conformation is extended and non-coplanar rather than compact, confirming Gregory et al.'s (1987) comments that an earlier 'parachute' model of folded back arms proposed by Kilar et al. [15] is unlikely.

5.5. Hingeless mutant: IgGMcg

The hingeless mutant IgGMcg has a P_{exp} value 1.20 ± 0.03 that is a little lower than that for the related IgG4 and IgG2. Such a P value from SOLPRO can be generated by taking the models of Fig. 8 and returning the twist angle α of Fc relative to the Fab domains from 90° to 0° to give the coplanar model of Fig. 11a with SOLPRO $P = 1.20$. Alternatively the twist angle α can be retained at 90° and the angle between the Fab arms ϕ stretched out to 180° (Fig. 11b). A model where both $\phi = 180$ and the twist angle $\alpha = 0$ gives too low a SOLPRO P value (1.17, Fig. 11c). Of the two models in Fig. 11a,b, Fig. 11a is most consistent with the coplanar crystal structure for IgGMcg of Rajan et al. [36] — see also Guddat et al. [37].

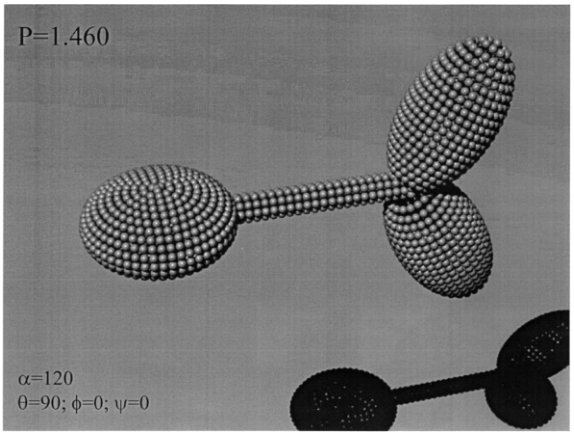

Fig. 10. Model for IgG3 based on an increased hinge length of 30% compared with estimates from electron microscopy. This time agreement can be found between the model ($P = 1.46$) and the experimental $P = 1.46 \pm 0.04$.

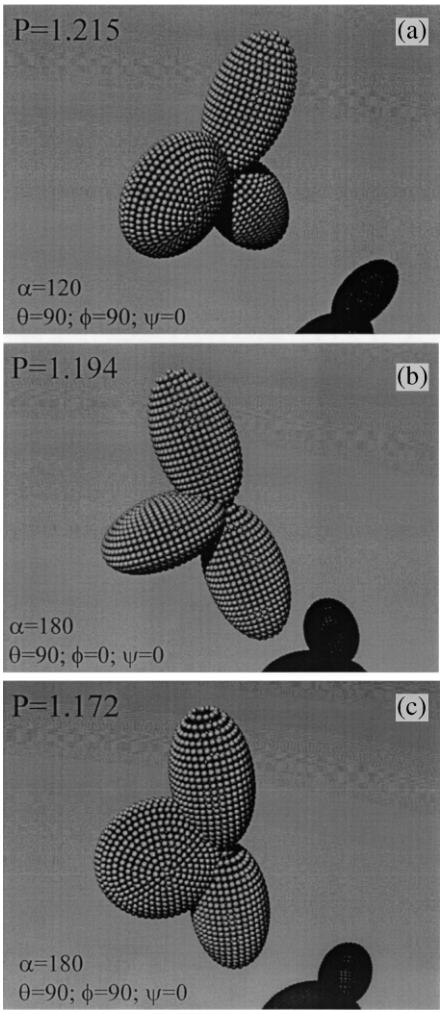

Fig. 11. Coplanar T- and Y-models for the hingeless mutant IgGMcg. The experimental value of $P = (1.23 \pm 0.03)$ is best satisfied by either model (a) (coplanar Y-shape, with twist angle, $\phi = 90$, $P = 1.215$), or with model (b), a coplanar T-shape, with twist $\phi = 0$ and $P = 1.194$.

5.6. Hingeless mutant: IgGDob

IgGDob is structurally very similar to that for IgGMcg, and yet its measured $s^{\circ}_{20,w}$ value, 6.30 ± 0.05 S, by both Gregory et al. [10] and in the present study is considerably lower than that for IgGMcg: the corresponding P_{exp} value is as a result very high 1.30 ± 0.02 and too high for any of the hingeless models. The only conclusion that can be drawn for this is that the measurements of the sedimentation coefficient were correct in both studies but the IgGDob protein had become somewhat aged/denatured: the IgGMcg work is therefore to be regarded as the definitive hydrodynamic study for a hingeless mutant.

6. Concluding remarks

The 'crystallohydrodynamic' approach of using known crystallographic data for individual domains of multi-domain proteins and then using these data in conjunction with solution data on the domains and intact structures to describe the low resolution time-averaged spatial orientation of the domains relative to each other appears to have been vindicated for the subclasses of the human IgG system of antibodies. The extension of this approach to other classes of antibody and also other multi-domain proteins such as chaperonins would also appear to be vindicated, at least for those multi-domain proteins where the individual domain structures are known. The procedure is as follows. (1) Surface ellipsoids are fitted to high resolution structures of the domains using the routine ELLIPSE [16–18]. (2) Universal hydrodynamic shape parameters are then specified exactly using ELLIPS2 [3], and also to a good approximation from surface shell models of spherical beads fitted to these ellipsoids using SOLPRO [24,25] (checked against the exact ellipsoid results). (3) Combination of a calculated universal shape parameter with the corresponding measured experimental parameter for each of the domains then yields an estimate for the (time-averaged) hydration of each domain and hence an average hydration for the whole molecule. (4) Combination of this value with the appropriate experimental hydrodynamic measurement(s) allows universal shape parameters to be specified for the whole molecule. (5) The appropriate spatial arrangements of the bead-shell domains can then be identified (using where appropriate a cylindrical hinge between the domains) which give universal shape parameters from SOLPRO consistent with (4).

Unfortunately, apart from the IgGMcg and Ig-

GDob hingeless mutants, there are, as far as we are aware, no crystal structures published for intact immunologically active human IgGs. There are, however, structures available for a mouse IgG1 [38] and a mouse IgG2a [39], both with only small hinge regions (unlike human IgG1) facilitating high resolution measurement. Interestingly, the overall conformation of the mouse IgG2a is a 'distorted-T' and IgG1 a 'distorted-Y', comparable with the solution conformations of human IgG2 and 4 in this study, whereas the hingeless IgGMcg is a symmetric or coplanar T-shape on the basis of both crystallographic (Guddat et al. [37]) and solution (this study) measurement.

6.1. Is the ellipsoid representation for the domains necessary?

An alternative approach would be to represent the domain crystal structure as an irregular array of surface beads, rather than an ellipsoidally smooth surface of beads. The hydrodynamics for ellipsoidal surfaces can however be described exactly, those for beads only approximately: the ellipsoid *then bead* stage gives the modeller a ready check on the magnitude of the error induced caused by the approximate hydrodynamics of beads: the error is normally very small. Further, hydrodynamics is not a high-resolution technique, and claims to the contrary need to be treated with considerable caution.

6.2. Should universal shape parameters such as P be used rather than the sedimentation coefficient directly?

Universal shape parameters [1,3,24] are shape parameters independent of size. So the Perrin 'frictional ratio due to shape' function P is a universal parameter since a given shape has a single value of P, whereas the sedimentation coefficient is not, since the value of the latter is affected by the molecular weight and volume (including hydration contributions) of the macromolecule. To experimentally measure P of course requires the sedimentation coefficient, molecular weight and an estimate for hydration [cf. Eqs. (1) and (2)]. The two schemes are entirely equivalent — in this application, however, use of the universal shape parameter P has allowed us to deal with hydration in a more convenient way: as a result all the representations of Figs. 3–11 could be given purely on a shape basis.

6.3. The more the number of measurements the merrier

As always, the more detail required, the greater the number of independent solution measurements is needed. This would also apply to studies seeking to detect subtle differences between molecular structure in the crystal and dilute solution states, a matter not the subject of the present study. Solution X-ray and neutron scattering would appear to provide a useful supplement, but as noted before potential beam damage and aggregation problems give rise to considerable uncertainty. More attractive options would appear to be rotational hydrodynamic probes of fluorescence depolarisation anisotropy decay and possibly the new generation of 'pressure imbalance' viscometers which facilitate measurement of the sensitive shape function known as the intrinsic viscosity (see Harding, [40]) without recourse to high concentration measurement and all its associated problems of aggregation and amounts of sample required. Combining shape parameters together (such as P with corresponding parameters from fluorescence anisotropy decay) provide a route for eliminating the apparent hydration from a requirement for experimental measurement [3,4]. Such a route is an attractive option, although such combined shape functions are generally less sensitive to shape variation and such a route makes the supposition that the 'apparent hydration' is the same for both measurements. Such procedures, using P or other functions can also say nothing about the dynamics of the hydration process: for that, other techniques — such as NMR — are required.

References

[1] S.E. Harding, Modelling the gross conformation of assemblies using hydrodynamics: the whole body approach, in: S.E. Harding, A.J. Rowe (Eds.), Dynamic

Properties of Biomolecular Assemblies, Royal Society of Chemistry, Cambridge, UK, 1989, pp. 32–56.
[2] S.E. Harding, On the hydrodynamic analysis of macromolecular conformation, Biophys. Chem. 55 (1995) 69–93.
[3] S.E. Harding, J.C. Horton, H. Cölfen, The ELLIPS suite of macromolecular conformation algorithms, Eur. Biophys. J. 25 (1997) 347–359.
[4] J. Garcia de la Torre, Hydrodynamic properties of macromolecular assemblies, in: S.E. Harding, A.J. Rowe (Eds.), Dynamic Properties of Biomolecular Assemblies, Royal Society of Chemistry, Cambridge, UK, 1989, pp. 3–31.
[5] B. Carrasco, J. Garcia de la Torre, Hydrodynamic properties of rigid particles: Comparison of different modeling and computational procedures, Biophys. J. 75 (1999) 3044–3057
[6] K.G. Davis, M. Glennie, S.E. Harding, D.R. Burton, A model for the solution conformation of rat IgE, Biochem. Soc. Trans. 18 (1990) 935–936.
[7] B. Carrasco, J. Garcia de la Torre, O. Byron et al., Novel size-independent modeling of the dilute solution conformation of the immunoglobulin IgG Fab′ domain using SOLPRO and ELLIPS, Biophys. J. 77 (1999) 2902–2910.
[8] P.G. Squire, M.E. Himmel, Hydrodynamics and protein hydration, Arch. Biochem. Biophys. 196 (1979) 165–177.
[9] F. Perrin, Mouvement Brownian d'un ellipsoide II. Rotation libre et depolarisation des fluorescences. Translation et diffusion de molecules ellipsoidales, J. Phys. Radium 7 (1936) 1–11.
[10] L. Gregory, K.G. Davis, B. Sheth, J. Boyd, R. Jefferis, C. Nave, D.R. Burton, The solution conformations of the subclasses of human IgG deduced from sedimentation and small angle x-ray scattering studies, Mol. Immunol. 24 (1987) 821–829.
[11] R. Sarma, A.G. Laudin, A three-dimensional structure of a human IgG1 immunoglobulin at 4 Å resolution; a computer fit of various structural domains on the electron density map, J. Appl. Cryst. 15 (1982) 476–481.
[12] E.W. Silverton, M.A. Navia, D.R. Davies, Three dimensional structure of an intact human immunoglobulin, Proc. Natl. Acad. Sci. USA 74 (1977) 5140–5144.
[13] J. Garcia de la Torre, V.A. Bloomfield, Hydrodynamic properties of macromolecular complexes, Biopolymers 16 (1977) 1747–1763.
[14] J. Pilz, E. Schwatz, W. Palm, Small angle x-ray studies of the human immunoglobulin molecule Kol, Eur. J. Biochem. 75 (1977) 195–199.
[15] F. Kilar, I. Simon, S. Lakatos, F. Vonderviszt, G.A. Medigyesi, P. Zavodsky, Conformation of human IgG subclasses in solutions: small angle X-ray scattering and hydrodynamic studies, Eur. J. Biochem. 147 (1985) 17–25.
[16] W.R. Taylor, J.M. Thornton, W.G. Turnell, An ellipsoidal approximation of protein shape, J. Mol. Graphics 1 (1983) 30–38.
[17] S. Hubbard, PROTRUDER: a FORTRAN Program to Calculate an Equi-momental Ellipsoid and Make Protrusion Index Calculations, University College, London, 1994.
[18] R.A. Laskowski, SURFNET: a program for visualizing molecular surfaces, cavities and intermolecular interactions, J. Mol. Graph. 13 (1995) 323–330.
[19] H.K. Schachman, Ultracentrifugation in Biochemistry, Academic Press, New York, 1959.
[20] W.D. MacMillan, Dynamics of Rigid Bodies, McGraw-Hill, New York, 1936, pp. 31–52.
[21] J.L. Synge, B.A. Griffin, Principles of Mechanics, McGraw-Hill, New York, 1959, pp. 282–294.
[22] R.L. Brady, D.J. Edwards, R.E. Hubbard et al., Crystal structure of a chimaeric Fab′ fragment of an antibody binding tumour cells, J. Mol. Biol. 227 (1992) 253–264.
[23] J. Deisenhofer, Crystallographic refinement and atomic models of a human Fc fragment and its complex with fragment B of protein from *Staphylococcus aureus* at 2.9 and 2.8 angstroms resolution, Biochemistry 20 (1981) 2361.
[24] J. Garcia de la Torre, B. Carrasco, S.E. Harding, SOLPRO: theory and computer program for the prediction of SOLution PROperties of rigid macromolecules and bioparticles, Eur. Biophys. J. 25 (1997) 361–372.
[25] J. Garcia de la Torre, S.E. Harding, B. Carrasco, Calculation of NMR relaxation, covolume and scattering-related properties of bead models using the SOLPRO computer program, Eur. Biophys. J. 28 (1999) 119–132.
[26] D.W. Cleavland, S.G. Fisher, M.W. Kirschner, U.K. Laemmli, Peptide mapping by limited proteolysis in sodium dodecyl sulfate and analysis by gel electrophoresis, J. Biol. Chem. 252 (1977) 1102–1106.
[27] D.R. Burton, L. Gregory, R. Jefferis, Aspects of the molecular structure of IgG subclasses, Mongr. Allergy 19 (1986) 7–35.
[28] R. Giebeler, The Optima XL-A: a new analytical ultracentrifuge with a novel precision absorption optical system, in: S.E. Harding, A.J. Rowe, J.C. Horton (Eds.), Analytical Ultracentrifugation in Biochemistry and Polymer Science, Royal Society of Chemistry, Cambridge, UK, 1992 Ch. 2.
[29] J.S. Philo, An improved function for fitting sedimentation velocity data for low-molecular-weight solutes, Biophys. J. 72 (1997) 435–444.
[30] J. Behlke, O. Ristau, Molecular mass determination by sedimentation velocity experiments and direct fitting of the concentration profiles, Biophys. J. 72 (1997) 428–434.
[31] W.F. Stafford, Boundary analysis in sedimentation transport experiments: a procedure for obtaining sedimentation coefficient distributions using the time derivative of the concentration profile, Analyt. Biochem. 203 (1992) 295–301.
[32] S.J. Perkins, Protein volumes and hydration effects. The calculations of partial specific volumes, neutron scatter-

ing matchpoints and 280 nm absorption coefficients for proteins and glycoproteins from amino acid sequences, Eur. J. Biochem. 157 (1986) 169–180.

[33] N. Gralén, Sedimentation and Diffusion Measurements on Cellulose and Cellulose Derivatives, Ph.D. Dissertation, University of Uppsala, Sweden, 1944.

[34] H. Cölfen, S.E. Harding, MSTARA and MSTARI: interactive PC algorithms for simple, model independent evaluation of sedimentation equilibrium data, Eur. Biophys. J. 25 (1997) 333–346.

[35] R. Pumphrey, Computer models of the human immunoglobulins: shape and segmental flexibility, Immun. Today 7 (1986) 174–178.

[36] S.S. Rajan, K.R. Ely, E.E. Abola et al., The 3-dimensional structure of the Mcg IgG1 immunoglobulin, Mol. Immunol. 20 (1983) 787–799.

[37] L.W. Guddat, J.N. Herron, A.B. Edmundson, 3-dimensional structure of a human-immunoglobulin with a hinge deletion, Proc. Natl. Acad. Sci. USA 90 (1993) 4271–4275.

[38] L.J. Harris, E. Skaletsky, E. McPherson, Crystallographic structure of an intact IgG1 monoclonal antibody, J. Mol. Biol. 275 (1998) 861–872.

[39] L.J. Harris, S.B. Larson, E. Skaletsky, A. McPherson, Comparison of the conformations of two monoclonal antibodies with hinges, Immunol. Rev. 163 (1998) 35–43.

[40] S.E. Harding, The intrinsic viscosity of biological macromolecules. Progress in measurement, interpretation and application to structure in dilute solution, Prog. Biophys. Mol. Biol. 68 (1997) 207–262.

[41] A. Schmidt-Kessen, A. Lustig, Comparison of IgG3 and IgG1 by ultracentrifugation, Hoppe-Seyler's Z. Physiol. Chem. 362 (1981) 18–19.